Comprehensive Conventional Analysis of Southern Hemisphere Coal Chars of Different Ranks for Fixed Bed Gasification

By Andrew O. Odeh

North-West University, South Africa

Abstract- In this study, the physical and chemical changes accompanied in the coal to char transition were examined by conventional and Fourier Transform infrared spectroscopy (FTIR) techniques. Six coals (lignite to anthracite) of ≤ 75 **μ**m were acid washed, and subjected to a slow heating rate of 20 °C/min from 450 to 700 °C at atmospheric atmosphere. The chars were characterized by physical, chemical and petrographic evaluations. The coals were low rank C lignite (Rov = 0.31), low rank B sub-bituminous (Rov = 0.47), medium rank C bituminous (Rov = 0.73 for high volatile and Rov = 0.78 for low volatile), high rank C semi-anthracite (Rov = 2.48) and high rank B anthracite (Rov = 3.26) respectively. Char properties determined by conventional technique (proximate, ultimate and calorific value) and FTIR revealed correlations of the chemical structural changes during the coal to char transition. Unique relationships between the fuel ratio and other coal properties (H/C atomic ratio and aromaticity) were established. The fuel ratio was determined to be in the range of 1.9 – 21.0 for lignite; 3.4 – 20.3 for sub-bituminous; 5.5 – 24.0 for bituminous; 11.6 – 29.6 for semi-anthracite and 16.5 – 27.8 for anthracite.

Keywords: southern hemisphere coal; char transition; pyrolysis; fuel ratio; rank parameter; FTIR.

GJRE-E Classification : FOR Code: 290899

COMPREHENSIVECONVENTIONALANALYSISOFSOUTHERNHEMISPHERECOALCHARSOFDIFFERENTRANKSFORFIXEDBEDGASIFICATION

Strictly as per the compliance and regulations of :

Comprehensive Conventional Analysis of Southern Hemisphere Coal Chars of Different Ranks for Fixed Bed Gasification

Andrew O. Odeh

Abstract- In this study, the physical and chemical changes accompanied in the coal to char transition were examined by conventional and Fourier Transform infrared spectroscopy (FTIR) techniques. Six coals (lignite to anthracite) of ≤ 75 μm were acid washed, and subjected to a slow heating rate of 20 ºC/min from 450 to 700 ºC at atmospheric atmosphere. The chars were characterized by physical, chemical and petrographic evaluations. The coals were low rank C lignite (Rov = 0.31), low rank B sub-bituminous (Rov = 0.47), medium rank C bituminous (Rov = 0.73 for high volatile and Rov = 0.78 for low volatile), high rank C semi-anthracite (Rov = 2.48) and high rank B anthracite (Rov = 3.26) respectively. Char properties determined by conventional technique (proximate, ultimate and calorific value) and FTIR revealed correlations of the chemical structural changes during the coal to char transition. Unique relationships between the fuel ratio and other coal properties (H/C atomic ratio and aromaticity) were established. The fuel ratio was determined to be in the range of 1.9 – 21.0 for lignite; 3.4 – 20.3 for sub-bituminous; 5.5 – 24.0 for bituminous; 11.6 – 29.6 for semi-anthracite and 16.5 – 27.8 for anthracite.

It was possible to find a first-order relationship between the char aromaticity and atomic H/C.

Keywords: *southern hemisphere coal; char transition; pyrolysis; fuel ratio; rank parameter; FTIR.*

I. INTRODUCTION

Pyrolysis remains an important process for thermo-chemical coal conversion either as an individual process for char and tar/oil production or as a step in other coal conversion processes such as combustion, gasification, and liquefaction. During fixed bed gasification, coal passes through four distinct stages: drying, pyrolysis, reduction, and combustion [1]. In the pyrolysis stage, volatiles devolatilization occurs and the properties transformation from coal to char can be dramatic for some coals. The behavior of coal under pyrolysis can be linked to coal properties and process conditions such as coal rank, particle size, porosity, surface area, mineral content, petrographic composition, process temperature, process pressure, catalyst, and heating rate [2 – 13]. Thus, among other aspects the time-temperature histories will have an influence on the char reactivity and behavior. The

Author: Coal Research group, Unit of Energy Systems, School of Chemical and Minerals Engineering, North-West University, e-mail: odehandy@yahoo.com

inorganic components are sometime responsible for poor and unstable performance of coal conversion processes [8, 14 - 17]. However, in other conversions, such as direct liquefaction the pyrite mineral is beneficial to the yield of the process [3, 12].

The atomic H/C, aromaticity, petrography, and fuel ratio (the ratio of fixed carbon to volatile matter content) influences on coal conversion processes have been investigated [18-33]. Char properties such atomic H/C ratio, aromaticity, morphology and fuel ratio has also received attention [8, 19, 25, 34 – 36]. However, a systematic evaluation for the transitions accompanying slow-heating rate using a temperature monitored process is limited [37-40]. Zhao et al. [37] examined the pyrolysis behaviour of vitrinite and inertinite extracts from a Chinese bituminous coal at temperatures of 400 to 650 ºC and heating rate of 10 ºC/min and reported that the atomic H/C ratio of both the vitrinite and inertinite char decreased with increasing temperature, and have similar atomic H/C ratio and structure characteristics at the final temperature. Guerrero et al. [38] performed combined reflectance analysis on heat-treated coal at temperatures of 400, 450, 550, 750, 1000 ºC and reported the effect of volatiles release on the optical properties of macerals from different ranks The reflectance of coal macerals increases with increasing pyrolysis temperature, with temperature being the most relevant factor in determining the reflectance of inertinite macerals. The studies of Jimenez et al. [39] and Alonso et al. [40] both focused on the influence of process conditions on char optical texture and reactivity. They reported the influence of both pressure and temperature on the resultant chars. The coal char properties derived at 900 ºC and heating rate of 20 ºC/min, exhibited significant changes in reactivity in the pressure range 0.1 to 0.5 MPa, after which no significant changes were observed with pressure increment. Alonso et al. observed that the temperature of pyrolysis performed at temperatures of 1000 and 1300 ºC had a strong effect on char reactivity, which was attributed to inertinite maceral in high rank coals yielding both more reactive and less reactive materials depending on the process conditions. Tracing char structure evolution during coal conversion process allows an improved evaluation of the conversion mechanism [38]. Of the many rank

indicators and char properties the fuel ratio (a commonly used factor in the design of unit operations for coal conversion processes and also a useful parameter in the selection of coals used in coal blending plant) has not commonly evaluated but may prove to be useful indicator in the coal to char conversion process [3, 7]. Most power plants utilized coals with fuel ratio in the range of 1.0 - 2.5 due to their combustion characteristics of calorific values, ignitability, and combustibility [4, 7, 33]. Fuel ratio is considered to give an indication of coal reactivity as coals with fuel < 1.5 are thought to combust more smoothly whereas coal with fuel ratio > 1.5 combust with difficulty [2, 4, 31]. Kurose et al. [4] examined the pulverized coal combustion characteristics of high-fuel-ratio coals with fuel ratio in the range of 1.46 to 7.10 and concluded that as the fuel ratio increases, nitrogen oxides (NO_x) emission reduces significantly and that the char's external surface area decreases with increase in the fuel ratio of the coal. Fuel ratio of acid washed and slow-heating coals are not readily available. Thus the fuel ratio is a somewhat forgotten rank parameter that may have utility in coal to char transitions.

Here the chemical and structural changes accompanying coal pyrolysis performed on a 75 μm size, at a heating rate of 20 °C/min from 450 to 700 °C at atmospheric pressure. The changes in the char structure were traced and relationship between char formation process indices and coal/char properties are established. The selected coals were acid washed to reduce mineral matter and ash influences.

II. Experimental

a) Sample Preparation

Six coals of varying rank were used: a lignite coal from Germany (LIG); a sub-bituminous coal from Nigeria (SUB); two South African bituminous coals (one is low volatile bituminous (BIT-LV) and the other, high volatile bituminous coal (BIT-HV); South African semi-anthracite (SA); and anthracite from South Africa (ANT). The coal samples were pulverized to coal particle size of ≤ 75 μm by employing a mechanical size reduction jaw crusher (Samuel Osborne (SA) LTD, model: 66YROLL) and a Fritsch P-14 rotary mill containing ceramic balls (Model number: 46 – 126). The required particle size of -75 μm was finally obtained from screening the particles from the rotary mill using a 75 μm screen All the samples were stored under argon in sealed bags.

The prepared coal samples were acid washed by sequential leaching with hydrofluoric acid (HF) and hydrochloric acid (HCl) as detailed in Strydom et al. [17].The HF (48%) and HCl (32%) were obtained from Associated Chemical Enterprise (ACE), South Africa.

b) Apparatus and procedure

The coal samples (40g) were placed in a ceramic boat in a horizontal tube furnace at atmospheric conditions initially. The samples were flushed with nitrogen (AFROX, ultra high purity grade) at atmospheric conditions, to remove oxygen from the oven for 15 min. at a flow rate of 1 litre/min. The furnace was then heated at 20 °C/min to the target temperature, and held isothermally for 60 minutes. The target temperature ranged from 450 to 700 °C, while keeping the samples under a nitrogen atmosphere. The char samples were stored in sealed bags.

The calorific value and conventional chemical analyses (proximate and ultimate analyses) of the untreated coal, acid treated and heat treated samples were performed according to the ISO 1928, ASTM 3172 and ASTM 3176 standards respectively at Advanced Coal Technology (ACT), Pretoria, South Africa. The surface areas of the various samples were determined using the carbon dioxide adsorption BET method on a Micromeritics ASAP2020 surface area analyser [41]. Prior to CO_2 adsorption, the samples (about 0.20 g) were degassed under vacuum (10.0 μmHg), for 48 hours at 25 and 380 °C for the coals and chars respectively. The evacuated sample was analysed at 0 °C in an ice bath. The results were processed using the Accelerated Surface Area and Porosimetry System (ASAP) 2020 software linked to the Surface Area Analyzer. The spectra used in obtaining the structural properties of both the coal and char were obtained from the Fourier-transform infrared spectrometer equipped with an attenuated total reflectance (FTIR-ATR), model Perkin-Elmer Spectrum 400. The procedure of FTIR-ATR as detailed by Li et al. was used [42]. Aromaticity (f_a) was obtained from the ratio of aromatic bands in the 900 – 700 cm^{-1} region to the aliphatic and aromatic bands in the 3000 – 2815 cm^{-1} region [43]. The vitrinite reflectance of the parent coal was obtained following the procedure and equipment at the coal and carbon laboratory, University of the Witwatersrand, South Africa as detailed in Malumbazo et al. [29].

III. Results and Discussion

Chemical analysis for the parent coal are summarized in Table 1, where coals are listed by increasing rank (lignite to anthracite) as determined by vitrinite reflectance analysis [29]. The rank parameters follow the expected trend with increasing rank, a decrease in volatile matter, hydrogen content, oxygen content, atomic O/C ratio and atomic H/C ratio, and an increase in carbon content, fuel ratio, and aromaticity [8 – 9, 12 – 15, 18 – 22, 54 – 55]. The atomic ratio of hydrogen to carbon (H/C) increases as the coal rank decreases with lignite coal sample having the highest ratio of 1.12 and the anthracite coal has the lowest

value of 0.36. A similar trend was obtained for the atomic O/C ratio with the lignite coal having a value of 0.20 and the anthracite coal, 0.02. The values obtained in this study compare well with those of Ibarra et al. [18], who reported values ranging from 1.27 for peat to 0.17 for anthracite for the atomic H/C ratio and 0.43 for peat and 0.06 for anthracite. The aromaticity shows a trend of increasing values with increasing coal rank with the lignite coal having a value of 0.38 and the anthracite a value of 0.97 [17 – 18, 25]. A similar trend was obtained for the calorific value with the lignite having a value of 21.2 MJ/kg and the anthracite a value of 29.6 MJ/kg. Typically there is a slight drop in the calorific value between the low rank and high rank coals. The fuel ratio ranges from 0.6 for the lignite coal to 16 for the anthracite coal. There was good agreement with the aromaticity, calorific value, and fuel ratio of the bituminous coals (BIT-LV and BIT-HV) with those reported by Everson et al. for typical South African bituminous coals [25].

The lignite coal has a mean random vitrinite reflectance of 0.35 representing a low rank C coal (Table 1). The mean random vitrinite reflectance obtained for the sub-bituminous coal in this study was 0.47 characterised as low rank B coal; for the bituminous coals, the values determined are 0.73 and 0.78 for BIT-LV and BIT-HV characterised as medium rank C coals. The high rank coals SA and ANT have values of 2.48 and 3.26 thus high rank C and high rank B coals respectively [28 - 29].

The chemical analyses of the acid-washed coal are presented in Table 2. The differences observed between parent and acid washed coal was significant. A similar trend was observed for the acid washed coals as was with the parent coals. Observations of increased surface area with coal rank for acid cleaned were also reported by Kister et al. [12] The increased volatile matter as a result acid washing was expected to have increased the surface area and porosity of the coals due to the opening of pores, which were blocked by mineral impurities, but that was not the case with lower rank coals that experienced higher percentage increase in volatile matter content [12]. However, that was not observed for the low-rank coals where the surface area was reduced or unchanged. Mahajan and Walker [16] also observed a reduction in surface area for some coals, attributed to mineral precipitation or blocking of pores. This finding of insignificant change in aromaticity was reported by the work of Strydom et al. [17], who reported no change in the aromaticity of the demineralized coals when compared to the raw bituminous coals, and by the work of Ishihara et al. [33], who investigated the effect of demineralization on hydrogen transfer of coal with tritiated gaseous hydrogen. They revealed that demineralization does not affect the amounts of functional groups in the parent

coals of different ranks ranged from lignite to low volatile bituminous coal. Here, the atomic H/C was not significantly changed and the O/C was relatively constant after the acid wash. This is similar to the observations of Strydom et al. [17] and Kister et al. [12].

Table 3 shows the atomic H/C ratio decreases with increasing char formation temperature. At temperature of 700 °C, there was a convergence to the value of 0.13 which was also observed by Zhao et al. [37]. As can be seen in Table 3, the O/C atomic ratio decreases with increasing char formation temperature for all the coals apart from anthracite with constant value of 0.03 for the temperature range of 450 – 700 °C. The uniform value obtained for the anthracite can be explained by variation in petrographic composition (data not included in this paper). The anthracite may be considered as a typical South African high-inertinite content coal. The aromaticities show an increasing trend with increasing char formation temperature (Table 3). For instance, Everson et al. [25] had similar aromaticities and trends for raw and acid-washed chars heat treated in a similar range (550 to 850 °C).

The fuel ratio data is given in Table 3. The fuel ratio increases with increase in the char formation temperature process. Though slight differences can be observed in the values obtained for the parent coal and the acid washed coals, the impart is more significant in the heat treated coal and a convergence occur around 700 °C especially for the low and medium ranks (Table 3). During the char formation process in the temperature 450 – 700°C, devolatilization, aromatization, and arrangement of the basic structural units (BSUs) are likely to have occurred as there were significant transformational changes in aromaticity, fuel ratio, H/C and O/C obtained. The pattern of these transformations in aromaticity, fuel ratio and H/C was consistent for all coal chars: lignite to anthracite. The H/C values decreases with increase in the heating temperature while the aromaticity and fuel ratio increases with increase in heating temperature as seen in Figure 1. This is attributed to the chemical modification (devolatilization, removal of aliphatic groups and heteroatoms) that occurs during carbonization that results in the ordering of the internal structure of the samples [25, 43 – 45]. From these parameters it can be observed that coal increases its aromaticity and fuel ratio with increasing char formation temperature. Aromaticity and atomic H/C ratio are in use as reference indicators in coal conversion processes. It is suggested that fuel ratio has similar utility.

To establish a relationship between the determined aromaticity, fuel ratio and H/C ratio during the char formation temperatures of 450 – 700 °C; figures of the transitional relationships with

temperature, aromaticity with atomic H/C, fuel ratio versus aromaticity, fuel ratio versus H/C were constructed (Fig. 1 - 7). In Fig. 1, the changes in fuel ratio, aromaticity and atomic H/C of the parent coals are compared with the chars obtained at increasing char formation temperature. The fractional increase in the fuel ratio was more pronounced in the low and medium ranks with increasing char formation temperature as expected. The same trend was observed for the aromaticity, whereas, for the atomic H/C, fractional decrease was observed. Fig. 2 and 3 reveals the relationship between the aromaticity and atomic H/C ratio. The correlation between the aromaticity and H/C ratio gave a linear relationship (Fig.2), whereas for the coal char, the relationship obtained was dependent on the coal rank (Fig.3). These results are consistent with the general trends reported in previous studies for raw bituminous coal but the extension of these correlations to interpret the structural transformation of other coal rank remain a subject of controversy [46 -49]. Whereas the correlation obtained in this study is dependent on coal rank and could be used for the interpretation of the relationship between aromaticity and atomic H/C structural changes (Fig. 3). Fig.4 demonstrates the correlation between aromaticity and fuel ratio with increasing char formation temperature, which follows same trend for all coal ranks apart from the low rank coals with little degree of deviation from the trend. This deviation could be attributed to the higher percentage of oxygen and oxygen containing functional groups in the low rank coals (LIG and SUB). It is known the low-rank coals have limited thermoplastic ability and hence do not undergo as extensive an ordering as bituminous coals The two low-rank coals do not align and coalesce to the same degree resulting in a lower aromaticity. These results of increasing aromaticity with increasing char formation temperature are consistent with the general

trend reported in previous charring studies on raw coal in respect of increasing aromaticity with decreasing coal reactivity [50]; increasing aromatic condensation [51]; less ordered material [52]; increasing reflectance [32]; and increasing optical texture [38]. Fig.5 presents the variation of fuel ratio with atomic H/C. With increasing fuel ratio with the char formation temperature, there is a corresponding decrease in the atomic H/C with a convergence to the same value of 0.13 at the final char formation temperature of 700 °C. The fuel ratio for the two low rank coals were close with similar devolatilization behavior, the two bituminous coals with close fuel ratio values have a similar devolatilization behavior, while the two high rank coals behave in like manners when subjected to heat treatment.

Table 3 also shows the surface area decreasing with increasing rank in the char formation process. Figs. 6 indicates the variation of the BET surface area with the atomic O/C (lignite coal is used as an example for illustration) and % change in BET surface area with % change in oxygen (daf). The variation in atomic O/C and % change in oxygen and compared to the raw coal is more pronounced in the low rank coals, due to higher oxygen content and of oxygen-containing functional groups such as carboxylic and phenolic [19, 53-54]. Coal particles undergo thermo-chemical decomposition with release of volatile will often increase in the porosity and surface area of the resultant char [52, 55-57]. The relationship in Fig. 6 showed that for every decrease in the atomic O/C, there is a corresponding increase in the surface area during the char formation process. It is generally known that the diffusion of oxygen to and within the char particle influences the rate of char burning and resulting transitions in char morphology (Fig.5.) [19, 40, 58–59].

Table 1: Proximate analysis, ultimate analysis, calorific values, aromaticity, BET surface area, vitrinite reflectance and calculated H/C and fuel ratio values for untreated coal

Coal	LIG	SUB	BIT-LV	BIT-HV	SA	ANT
Inherent moisture(air dried) wt.%	15.4	9.6	4.2	2.1	1.0	1.5
Ash (air-dried) wt.%	12.4	9.0	29.1	16.2	17.3	11.2
Volatile matter (air-dried) wt.%	45.7	37.6	21.4	26.7	7.6	5.3
Fixed carbon (air-dried) wt.%	26.4	43.8	45.3	55.0	74.1	82.0
Carbon (daf) wt.%	70.5	75.6	77.5	81.6	90.4	90.2
Hydrogen (daf) wt.%	6.6	5.2	4.5	4.6	3.5	2.7
Nitrogen (daf) wt.%	0.6	1.7	2.2	2.0	2.0	2.2
Oxygen (daf) wt.%	18.5	16.9	15.4	10.7	3.3	2.7
Sulphur (daf) wt.%	3.7	0.7	0.4	1.2	0.9	2.3
Gross calorific value (MJ/kg) (air-dried)	21.2	24.6	20.0	26.8	28.7	29.6
H/C (daf).	1.12	0.82	0.69	0.67	0.46	0.36
O/C (daf)	0.20	0.17	0.15	0.10	0.03	0.02
f_a	0.38	0.57	0.70	0.71	0.91	0.97
Fuel ratio	0.6	1.2	2.1	2.1	10	16
CO_2 BET surface area (m²/g)	74	104	95	84	108	122
Rank (mean random vitrinite reflectance %)	0.31	0.47	0.78	0.73	2.48	3.26

Table 2 : Proximate analysis, ultimate analysis, calorific values, aromaticity, BET surface area and calculated H/C and fuel ratio values for acid – washed coal

Coal	LIG	SUB	BIT-LV	BIT-HV	SA	ANT
Inherent moisture(air dried) wt.%	1.7	1.9	1.3	2.7	2.3	2.5
Ash (air-dried) wt.%	0.8	2.0	3.3	1.2	1.8	1.5
Volatile matter (air-dried) wt.%	60.3	43.2	25.0	27.2	9.6	6.8
Fixed carbon (air-dried) wt.%	37.3	53.0	70.4	68.9	86.3	89.2
Carbon (daf) wt.%	69.2	75.1	80.9	83.4	89.0	85.6
Hydrogen (daf) wt.%	6.2	5.2	4.2	4.6	3.3	2.4
Nitrogen (daf) wt.%	0.6	1.8	2.3	2.0	1.8	2.0
Oxygen (daf) wt.%	20.3	17.4	12.3	9.1	5.0	7.7
Sulphur (daf) wt.%	2.7	0.1	0.3	1.0	0.7	2.1
Gross calorific value (MJ/kg) (air-dried)	28.9	29.3	30.0	32.0	33.3	32.7
H/C (daf)	1.08	0.83	0.62	0.66	0.45	0.34
O/C (daf)	0.22	0.17	0.11	0.08	0.04	0.07
fa	0.40	0.58	0.74	0.72	0.84	0.98
Fuel ratio	0.6	1.2	2.8	2.5	9.0	13.0
CO2 BET surface area (m2/g)	74	94	111	95	125	138

Table 3: Proximate analysis, ultimate analysis, calorific values, aromaticity, BET surface area and calculated H/C and fuel ratio values for heat – treated coal

CHAR	Wt % (air dried)				Wt % (daf)					daf	daf		m²/g
LIG	Mois.	Ash	V.M	F.C	C	H	N	O	S	O/C	H/C	f_a	FR	BET
450	2.8	1.5	32.6	63.0	82.9	3.1	1.0	10.4	2.5	0.10	0.45	0.66	1.9	170
500	2.5	1.7	29.8	66.0	85.1	2.8	1.0	8.4	2.6	0.08	0.40	0.69	2.2	194
550	2.4	1.7	22.3	73.6	88.9	2.1	1.0	5.8	2.3	0.05	0.28	0.73	2.3	230
600	2.1	1.8	9.8	86.2	90.4	2.1	1.1	4.1	2.3	0.04	0.28	0.74	8.8	242
650	2.5	1.8	6.7	89.0	91.8	1.6	1.1	3.3	2.3	0.03	0.21	0.76	13.3	263
700	3.1	2.4	4.3	90.1	93.1	1.0	1.0	2.6	2.3	0.01	0.13	0.79	21.0	269
SUB														
450	3.2	2.7	24.2	69.9	84.9	3.2	2.2	9.2	0.5	0.08	0.45	0.75	2.9	156
500	3.1	2.3	22.5	72.1	87.3	2.7	2.3	7.2	0.5	0.06	0.38	0.78	3.2	183
550	3.0	1.9	21.7	73.3	89.7	2.4	2.3	5.1	0.5	0.05	0.32	0.81	3.4	184
600	3.2	2.4	13.3	81.1	91.3	2.0	2.3	4.1	0.5	0.04	0.26	0.84	6.1	234
650	3.6	2.5	8.8	85.1	92.0	1.5	2.2	3.9	0.5	0.03	0.16	0.87	9.7	238
700	4.0	2.5	4.4	89.1	93.1	1.0	2.0	3.4	0.5	0.03	0.13	0.90	20.3	240
BIT- LV														
450	1.5	3.6	14.6	80.3	88.1	3.1	2.1	6.4	0.4	0.06	0.42	0.84	5.5	137
500	1.3	3.7	12.5	82.5	89.7	2.7	2.2	5.1	0.3	0.05	0.36	0.88	6.6	154
550	1.0	3.6	9.5	85.9	89.7	2.3	2.1	5.5	0.3	0.05	0.31	0.90	9.0	199
600	0.8	3.6	7.7	87.9	89.6	2.0	2.1	5.5	0.3	0.05	0.27	0.93	11.4	200
650	0.8	4.1	5.5	89.6	91.7	1.5	2.1	4.3	0.3	0.04	0.20	0.97	16.3	215
700	1.0	4.2	3.8	91.0	92.6	0.7	2.3	4.1	0.3	0.03	0.09	1.00	24.0	224
BIT- HV														
450	0.9	1.3	13.9	84.0	88.1	3.3	2.1	5.7	0.8	0.05	0.45	0.83	6.0	130
500	1.1	1.1	11.4	86.4	89.0	2.9	2.1	5.4	0.7	0.04	0.39	0.86	7.6	159
550	0.9	0.9	8.6	89.6	91.3	2.6	2.2	3.4	0.5	0.03	0.34	0.89	10.2	184
600	0.9	1.1	7.3	90.7	92.1	2.2	2.1	3.1	0.5	0.03	0.29	0.92	12.4	206
650	0.9	1.2	5.0	92.9	93.1	1.7	2.1	2.5	0.6	0.02	0.22	0.95	18.6	215
700	0.9	1.1	3.9	94.1	95.5	1.1	2.0	0.9	0.6	0.01	0.14	1.00	24.1	225
SA														
450	0.6	1.5	7.8	90.1	89.5	3.0	1.9	4.8	0.8	0.04	0.40	0.94	11.6	138
500	0.7	1.6	6.6	91.1	90.8	3.0	1.8	7.9	0.8	0.07	0.40	0.95	13.8	148
550	0.5	1.2	5.7	92.6	91.4	2.6	2.0	3.2	0.8	0.03	0.34	0.98	16.2	170
600	0.5	1.0	4.8	93.7	91.4	2.1	1.9	3.8	0.8	0.03	0.28	1.00	19.5	187
650	1.2	1.3	3.7	93.8	92.5	1.6	1.9	3.1	0.8	0.03	0.21	1.00	25.4	195
700	0.9	1.3	3.2	94.6	92.9	1.0	1.9	3.4	0.8	0.03	0.13	1.00	29.6	197

ANT														
450	0.9	1.3	5.6	92.2	90.0	2.3	2.1	3.6	2.0	0.03	0.31	0.97	16.5	114
500	0.8	4.9	5.3	89.0	89.9	2.1	2.1	3.8	2.0	0.03	0.28	0.98	16.8	135
550	0.7	8.1	4.4	86.8	90.6	2.1	2.1	3.0	2.1	0.03	0.28	1.00	19.7	137
600	0.7	3.4	4.5	91.4	90.4	1.9	2.1	3.6	2.0	0.03	0.25	1.00	20.3	151
650	0.8	1.4	6.3	91.5	91.3	1.7	2.1	3.0	2.0	0.03	0.22	1.00	24.5	163
700	0.7	1.4	3.4	94.5	91.4	1.0	2.1	3.5	2.0	0.03	0.13	1.00	27.8	164

F.C fixed carbon; V.M. volatile matter; GCV gross calorific value; f_a aromaticity; FR fuel ratio; BET BET surface area.
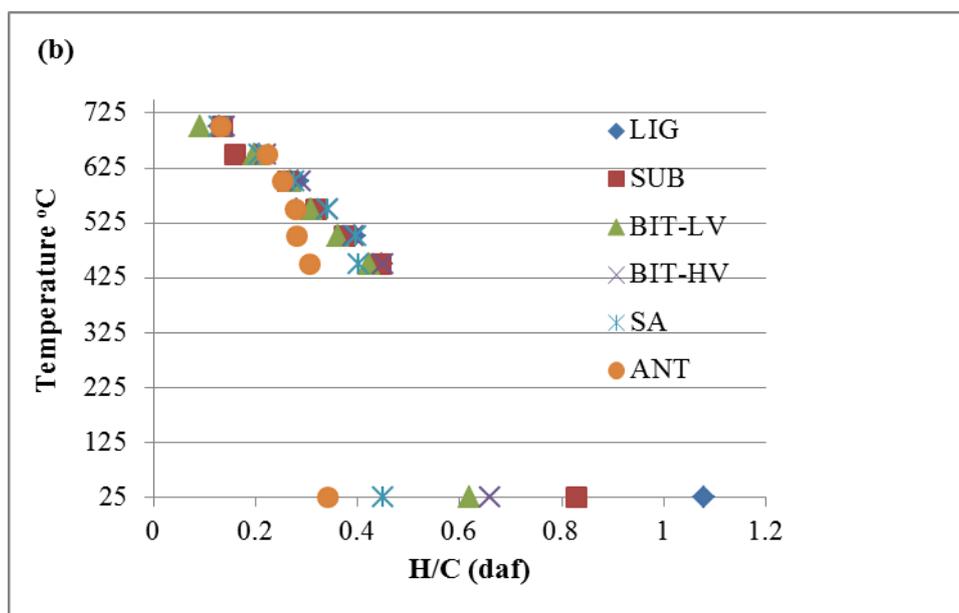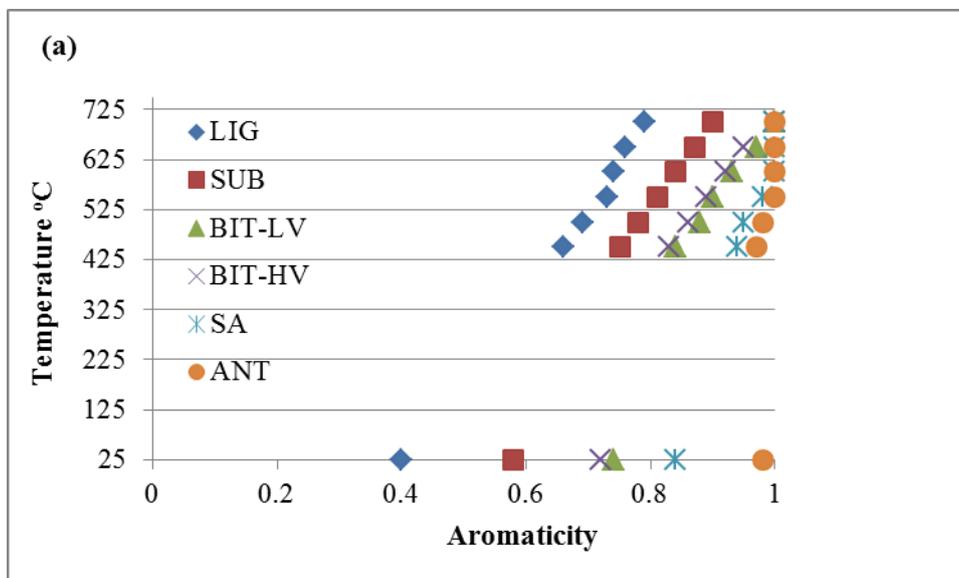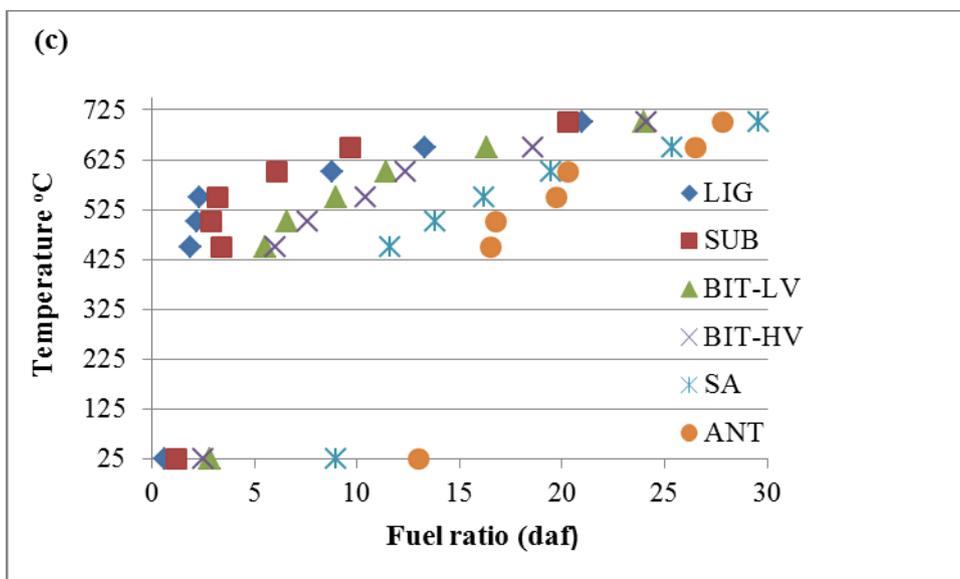
Fig. 1 : Transitional relationship between (a) Aromaticity; (b) H/C; (c) Fuel ratio with char formation temperature
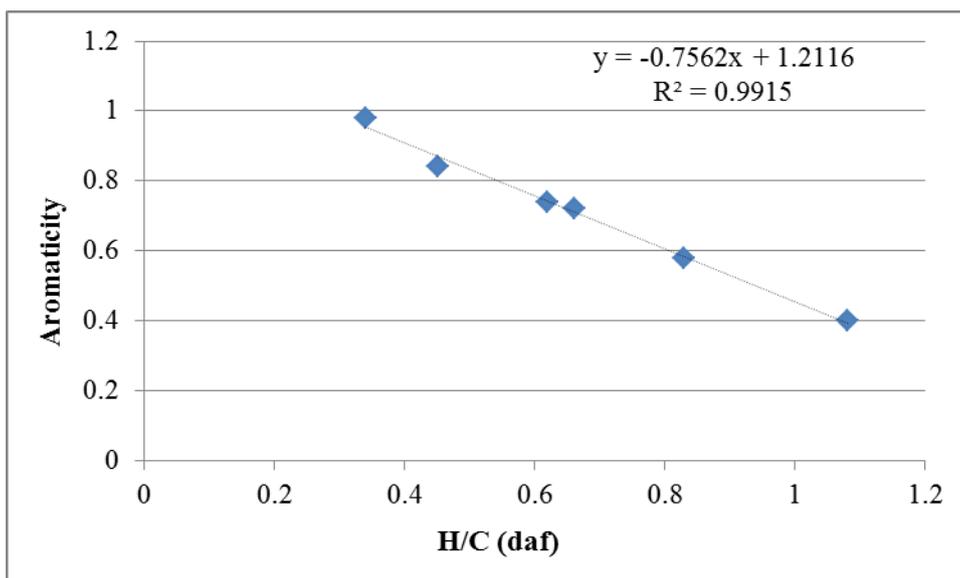
Fig. 2 : Relationship between the aromaticity and atomic H/C for the different coals
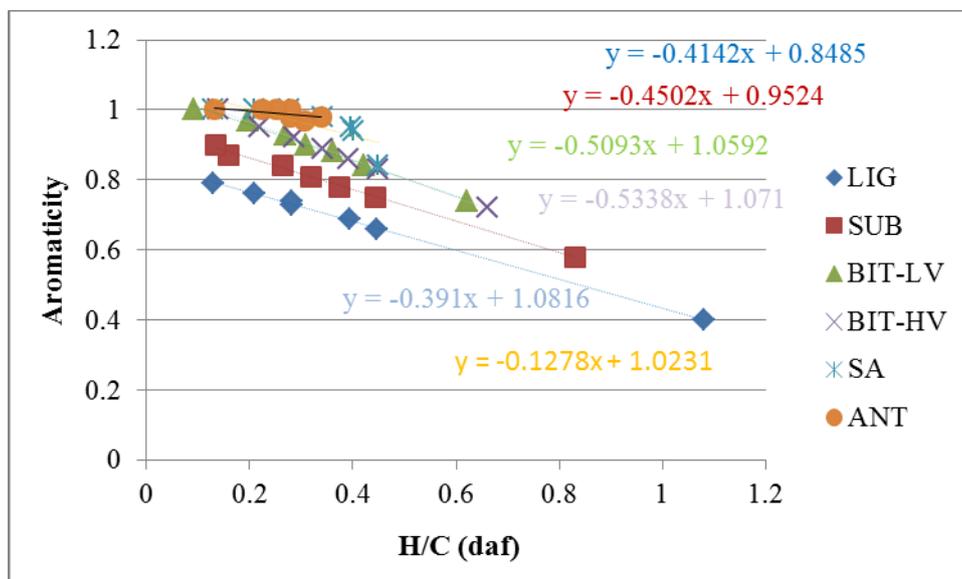
Fig. 3 : Relationship between the aromaticity and atomic H/C during pyrolysis
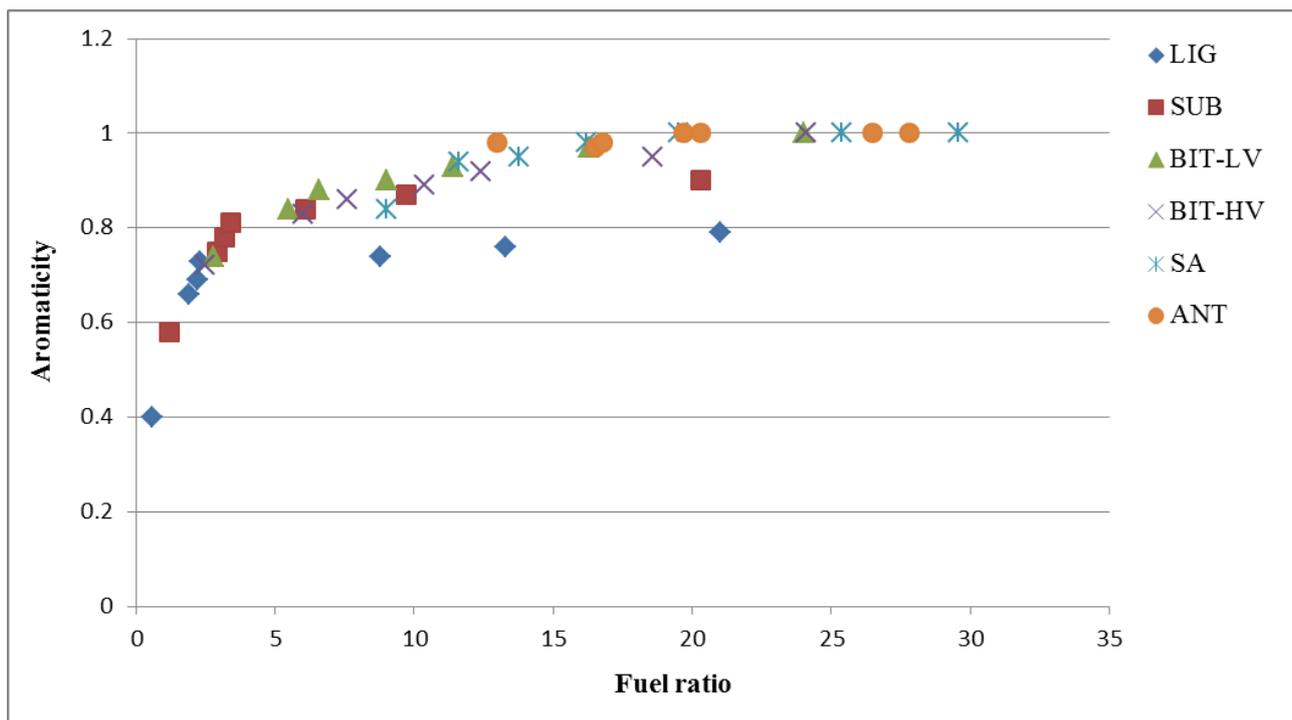
Fig. 4 : Transitional relationship between Aromaticity with Fuel ratio during pyrolysis
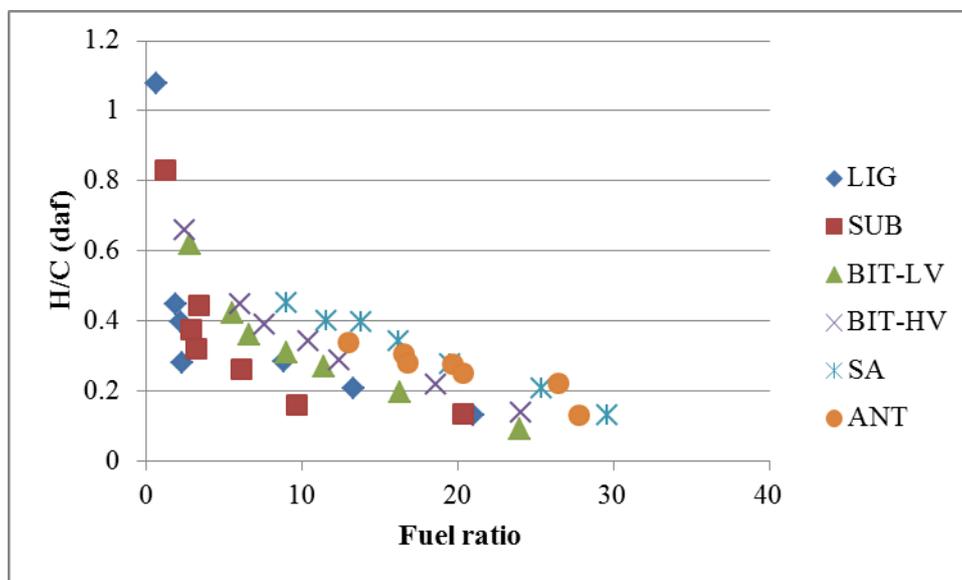
Fig. 5 : Transitional relationship between H/C and Fuel ratio during pyrolysis
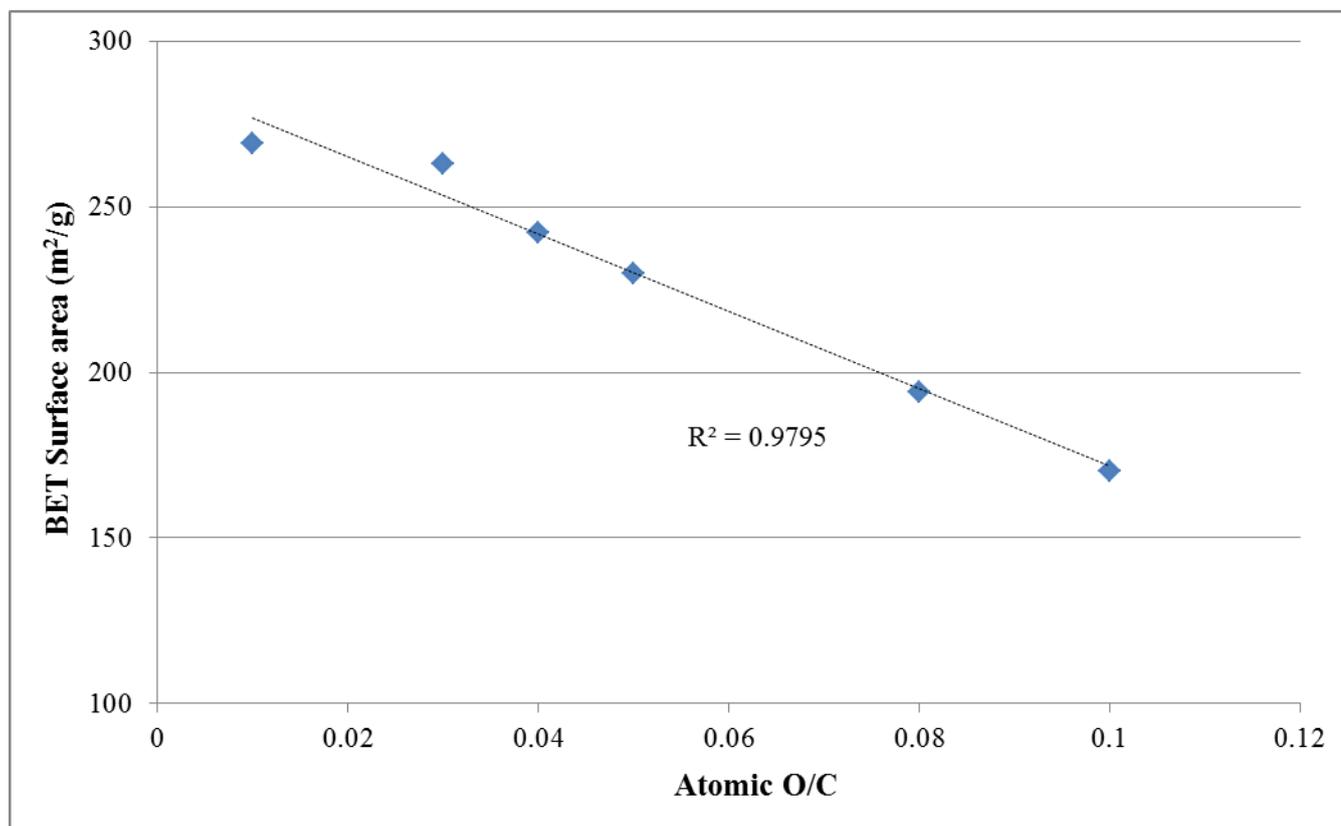
Fig. 6 : Variation of BET surface area with atomic O/C for the different acid-washed chars (450-700 ℃)

IV. CONCLUSION

Though previous research have reported the characterization of coal and the subsequent chars, analysis on the transition stage with emphasis on the organic component only have not been adequately investigated. This study entailed the characterization of coal and chars of different ranks using both conventional and FTIR technique. It can be concluded that all different rank of coals show a similar behaviour in char properties, when subjected to elevated temperatures. The volatile matter, hydrogen, oxygen, atomic O/C ratio and atomic H/C ratio, decrease with temperature, while the carbon, surface area, calorific

value, fuel ratio and aromaticity increase with charring temperature, with the low rank coals (LIG and SUB) showing larger fractional structural changes. The crystallite structure order here as measured by aromaticity for the acid washed coal chars increases slightly with increase in heat treatment temperature for the higher rank coals. Regardless of the rank, all the acid washed coal chars become increasingly similar in atomic H/C at 700°C. The same trend was revealed in the aromaticity for the medium to high rank coals at temperature of 700 °C. The data generated for the fuel ratio (1.9 – 21.0 for LIG; 2.9 – 20.3 for SUB; 5.5 – 24.0 for BIT-LV; 6.0 – 24.1 for BIT-HV; 11.6 – 29.6 for SA and 16.5 – 27.8 for ANT, respectively), may be considered as a useful resource in coal processing data base. Therefore, I suggest the fuel ratio as a somewhat forgotten rank parameter that has utility in char formation work to be reconsidered for this purpose. Finally, it was possible to find a linear relationship between the coal char aromaticity and atomic H/C.

V. Acknowledgement

References Références Referencias

1. Bunt JR, Wagner NJ, Waanders FB. Carbon particle type characterization of the carbon behavior impacting on a commercial-scale Sasol-Lurgi FBDB gasifier. Fuel 2009; 88: 771 - 779

2. Radovanovic M,. Jankes G. An approach to the use of fixed carbon – volatile matter graph. Fuel 1986; 65: 140 – 142.

3. Mazumdar, B.K. On the correlation of moist fuel ratio of coal with its spontaneous combustion temperature. Fuel 1996; 75: 646 – 648.

4. Kurose, R., Ikeda, M., Makino, H., Kimoto, M. and Miyazaki, T. 2004. Pulverized coal combustion characteristics of high-fuel-ratio coals. Fuel 83: 1777 – 1785.

5. Saxena SC. Devolatilization and combustion characteristics of coal particles. Progress in Energy Combustion and Science 1990; 16: 55 – 94.

6. Solomon PR, Serio MA, Suuberg EM. Coal pyrolysis: experiments, kinetic rates and mechanisms. Progess in Energy Combustion and Science 1992; 18: 133 – 220.

7. Niksa, S., Liu, G.-S. and Hurt, R.H. Coal conversion submodels for design applications at elevated pressures. Part I. Devolatilization and char oxidation. Progess in Energy and Combustion Science 2003; 29: 425 – 477.

8. Yu J, Lucas JA, Wall TF. Formation of the structure of chars during devolatilization of pulverized coals and its thermoproperties: a review. Progress in Energy and Combustion 2007; 33: 135 – 170.

9. Hunt R, Sun J.-K, Lunden M. A kinetic model of carbon burnout in pulverized coal combustion. Combustion and Flame 1988; 113: 181 – 197.

10. Wilkins RWT, George SC. Coal as a source of oil: a review. International Journal of Coal Geology 2002; 50: 317 – 361.

11. Ward CR, Li Z, Gurba LW. Comparison of the elemental composition of macerals determined by electron microprobe to whole-coal ultimate analysis data. International Journal of Coal Geology 2008; 75: 135 – 168.

12. Kister J, Guiliano M, Mille G, Dou H. Changes in the chemical structure of low rank coal after low temperature oxidation or demineralization by acid treatment. Fuel 1988; 67: 1076 – 1082.

13. Suggate RP, Dickinson WW. Carbon NMR of coals: the effects of coal type and rank. International Journal of Coal Geology 2004; 57: 1 – 22.

14. Vassilev SV, Vassileva CG, Karayigit AI, Bulut Y, Alastuey A, Querol X. Phase-mineral and chemical composition of fractions separated from composite fly ashes at the Soma power station, Turkey. International Journal of Coal Geology 2005; 61: 35 – 63.

15. Goodarzi F. Characteristics and composition of fly ash from Canadian coal-fired power plants. Fuel 2006; 85: 1418 – 1427.

16. Mahajan OP, Walker PL Jr.. Effect of inorganic matter removal from coal and chars on their surface area. Fuel 1979; 58: 333 – 337.

17. Strydom CA, Bunt JR., Schobert HH, Raghoo M. Changes to the organic functional groups of an inertinite rich medium rank bituminous coal during acid treatment processes. Fuel Processing Technology 2011; 92: 764 – 770.

18. Odeh, A. Comparative study of the aromaticity of the coal structure during the char formation process under both conventional and advanced analytical techniques. Energy & Fuels 2015, 29, 2676 – 2684.

19. Matsuoka K, Akahane T, Aso H, Sharma A, Tomita A. The size of polyaromatic layer of coal char estimated from elemental analysis data. Fuel 2008; 87: 539 – 545.

20. Odeh AO. Qualitative and quantitative ATR-FTIR analysis and its application to coal char of different ranks. Journal of Fuel Chemistry and Technology 2015; 43: 129 – 137.

21. Odeh, A. Exploring the potential of petrographics in understanding coal pyrolysis. Energy 2015, 87, 555 - 565.

22. Ibarra JV, Juan R. Structural changes in humic acids during the coalification process. Fuel 1985; 64: 650 – 656.

23. Chen KP. International A new mechanistic model for prediction of instantaneous coal outbursts – dedicated to the memory of Prof. Daniel D. Joseph. Journal of Coal Geology 2011; 87: 72 – 79.

24. Oboirien BO, Engelbrecht AD, North BC, du Cann VM, Falcon R. Textural properties of chars as determined by petrographic analysis: Comparison between air-blown, oxygen-blown and oxygen enriched gasification. Fuel 2012; 101: 16 – 22.

25. Everson RC, Okolo GN, Neomagus HWJP, dos Santos J-M. X-ray diffraction parameters and reaction rate modeling for gasification and combustion of chars derived from inertinite-rich coals. Fuel 2013; 109: 148 – 156.

26. Murchison DG. Petrographic aspects of coal structure: reactivity of macerals in laboratory and natural environments. Fuel 1991; 70: 296 – 315.

27. Komorek J, Morga R. Vitrinite reflectance property change during heating under inert conditions. International Journal of Coal Geology 2003; 54: 125 – 136.

28. Wagner NJ. The characterization of weathered discard coals and their behavior during combustion. Fuel 2008; 87: 1687 – 1697.

29. Malumbazo N, Wager NJ, Bunt JR. The petrographic determination of reactivity differences of two South African inertinite-rich lump coals. Journal of Analytical and Applied Pyrolysis 2012; 93: 139 – 146.

30. Kurose R, Ikeda M, Makino H. Combustion characteristics of high ash coal in a pulverized coal combustion. Fuel 2001; 80: 1447 – 1455.

31. Kurose R, Ikeda M, Makino H, Kimoto M, Miyazaki T. Pulverized coal combustion characteristics of high fuel ratios coals. Fuel 2004; 83: 1777 – 1785.

32. Gürdal G, Yalçin MN. Pore volume and surface area of the carboniferous coals from the Zonguldak basin (NW Turkey) and their variations with rank and maceral composition. International Journal of Coal Geology 2001; 48: 133 – 144.

33. Ishihara A, Sutrisna IP, Finahari I, Qian EW, Kabe T. Effect of demineralization on hydrogen transfer of coal with tritiated gaseous hydrogen. Fuel Processing Technology 2004; 85: 887-901.

34. Rosenberg P, Petersen HI, Thomsen E. Combustion char morphology related to combustion temperature and coal petrography. Fuel 1996; 75: 1071 – 1082.

35. Matsuzawa Y, Ayabe M, Nishino J, Kubota N, Motegi M. Evaluation of char fuel ratio in municipal pyrolysis waste. Fuel 2004; 83: 1675 – 1687.

36. Tang LG, Gupta RP, Sheng CD, Wall TF. The estimation of char reactivity from coal reflectogram. Fuel 2005; 84: 127 – 134.

37. Zhao Y, Hu H, Jin L, He X, Wu B. Pyrolysis behavior of vitrinite and inertinite from Chinese Pingshuo coal by TG-MS and a fixed bed reactor. Fuel Processing Technology 2011; 92: 780-786.

38. Guerrero A, Diez MA, Borrego AG. Effect of volatile matter release on optical properties of macerals from different rank coals. Fuel 2013; 114: 21-30.

39. Jimenez F, Mondragon F, Lopez D. Structural changes in coal chars after pressurized pyrolysis. Journal of Analytical and Applied Pyrolysis 2012; 95: 164-170.

40. Alonso MJG, Borrego AG, Alvarez D, Parra JB, Menendez R. Influence of pyrolysis temperature on char optical texture and reactivity. Journal of Analytical and Applied Pyrolysis 2001; 58-59: 887-909.

41. Hattingh BB, Everson RC, Neomagus HWJP, Bunt JR. Assessing the catalytic effect of coal ash constituents on the CO_2 gasification rate of high ash, South African coal. Fuel Processing Technology 2011; 92: 2048 – 2054.

42. Li Z, Fredericks PM, Rintoul L, Ward CR. Application of attenuated total reflectance micro-Fourier transform infrared (ATR-FTIR) spectroscopy to the study of coal macerals: Examples from the Bowen Basin, Australia. International Journal of Coal Geology 2007; 70: 87 – 94.

43. Alvarez D, Borrego AG. The evolution of char surface area along pulverized coal combustion. Energy and Fuels 2007; 21: 1085 – 1091.

44. Supaluknari S, Larkins FP, Redlich P, Jackson WR. Determination of aromaticities and other structural features of Australian coals using solid state 13C NMR and FTIR spectroscopies. Fuel Processing Technology 1989; 23: 47 – 61.

45. Mazumdar BK. On the relationship between carbon aromaticities and H/C ratios for bituminous coals. Fuel 1999; 78: 1239 – 1241.

46. Maroto-Valer MM, Love GD, Snape CE. Relationship between carbon aromaticities and H/C ratios for bituminous coals. Fuel 1994; 73: 1926 – 1928.

47. Maroto-Valer MM, Andrésen JM, Snape CE. Verification of the linear relationship between between carbon aromaticities and H/C ratios for bituminous coals. Fuel 1998; 77: 783 – 785.

48. Orrego-Ruiz JA, Cabanzo R, Mejía-Ospino E. Study of Colombian coals using photoacoustic Fourier transform infrared spectroscopy. International Journal of Coal Geology 2011; 85: 307 – 310.

49. Cai H.-Y, Guell AJ, Chatzakis IN, Lim J.-Y, Dugwell DY, Kandiyoti R. Combustion reactivity and

morphological change in coal chars: Effect of pyrolysis temperature, heating rate and pressure. Fuel 1996; 75: 15 – 24.

50. McBeath AV, Smernik RJ. Variation in the degree of aromatic condensation of chars. Organic Geochemistry 2009; 40: 1161 – 1168.

51. Davis KA, Hurt RH, Yang NYC, Headley TJ. Evolution of char chemistry, crystallinity, and ultrafine structure during pulverized-coal combustion. Combustion and Flame 1995; 100: 31 – 40.

52. Pusz S, Duber S, Kwiecinska B. The study of textural and structural transformations of carbonized anthracites. Fuel Processing Technology 2002; 77: 173 – 180.

53. Bale HD, Carlson ML, Schobert HH. Thermal modification of the pore structure of a North Dakota lignite. Fuel 1986; 65: 1185 – 1189.

54. Suarez-Ruiz I, Garcia A.B. Optical parameters as a tool to study the microstructural evolution of carbonized anthracites using high-temperature treatment. Energy and Fuels 2007; 21: 2935 – 2941.

55. Alonso MJG, Borrego AG, Alvarez D, Kalkreuth W, Menendez R. Physicochemical transformations of coal particles during pyrolysis and gasification. Fuel 2001; 80: 1857 – 1870.

56. Alonso MJG, Borrego AG, Alvarez D, Menendez R. A reactivity study of chars obtained at different temperatures in relation to their petrographic characteristics. Fuel 1999; 78: 1501 – 1513.

57. Ahmed II, Gupta AK. Particle size, porosity and temperature effects on char conversion. Applied Energy 2011; 88: 4667 – 4677.

58. Perry ST, Hambly EM, Fletcher TH, Solum MS, Pugmire RJ. Solid state C NMR characterization of matched tars and chars from rapid coal devolatilization. Proceedings of the Combustion Institute 2000; 28: 2313 – 2319.

59. Solum MS, Pugmire RJ, Jagtoyen M, Derbyshire F. Evolution of carbon structure in chemically activated wood. Carbon 1995; 33: 1247 – 1254.